Nanoscale

Accepted Manuscript

This article can be cited before page numbers have been issued, to do this please use: P. Schweng, L. Pammer and R. T. Woodward, *Nanoscale*, 2026, DOI: 10.1039/D5NR04338G.

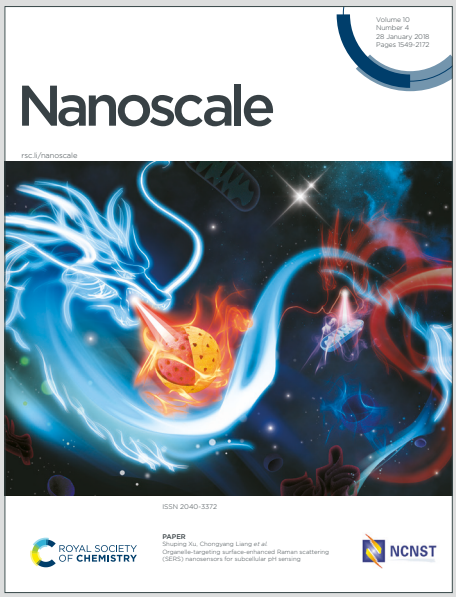

ROYAL SOCIETY OF CHEMISTRY

rsc.li/nanoscale

View Article Online
DOI: 10.1039/D5NR04338G

Elucidating the role of heteroatoms in hypercrosslinked polymer adsorbents for atmospheric water harvesting

Paul Schweng,[a,b] Lisa Pammer,[a] Robert T. Woodward[a]*

[a] Institute of Materials Chemistry and Research, Faculty of Chemistry, University of Vienna, Währinger Straße 42, 1090, Vienna, Austria

[b] Vienna Doctoral School in Chemistry, University of Vienna, Währinger Straße 42, 1090, Vienna, Austria

Keywords: Atmospheric water harvesting; separation and storage; hypercrosslinked polymers; porous organic polymers; adsorption;

Abstract

Hypercrosslinked polymers offer a promising platform for efficient adsorption-based atmospheric water harvesting, yet remain relatively unexplored. Here, we systematically introduce nitrogen, oxygen, sulfur, or sulfone moieties into hypercrosslinked polymer backbones to evaluate the impact of heteroatom inclusion on water sorption. Although the varying of the polymer skeleton significantly enhanced hydrophilicity, leading to total water capacity increases of up to 300%, heteroatom incorporation alone did not shift water uptake onsets to humidity levels relevant for atmospheric water harvesting. To address this, we also introduce sulfonate groups, which significantly improve both total water uptake and adsorption at low relative humidity. The best-performing material, SHCP-SO, achieves 0.69 $g \cdot g^{-1}$ uptake at 90% RH and 0.18 $g \cdot g^{-1}$ at 30% RH, with excellent long-term cycling stability. By tweaking network composition, our findings elucidate the role of various heteroatom sites and porosity for atmospheric water harvesting and unveil key porous organic polymer design principles.

View Article Online
DOI: 10.1039/D5NR04338G

Introduction

Water scarcity leaves more than 2.2 billion people without access to safely managed drinking water.[1] Rapid population growth and climate change continue to exacerbate this crisis, particularly in arid regions where traditional water sources are unreliable or polluted. Addressing this challenge requires new, scalable technologies that generate clean water from unconventional sources.

Atmospheric water harvesting (AWH) harnesses the vast reservoir of atmospheric moisture (1.3×10^{16} L globally), which holds significantly more water than all the world's freshwater rivers combined (2.1×10^{15} L).[2] Adsorption-based AWH utilises materials that passively capture water vapour from the air for re-release via controlled heat or humidity swings. The effectiveness of these adsorbents is dictated by key properties, including a high density of hydrophilic sites, large surface areas, fast adsorption–desorption kinetics, low heats of adsorption, and long-term chemical and thermal stability.[3]

Many existing AWH sorbents come with significant trade-offs. Common desiccants, such as zeolites and hygroscopic metal salts, uptake water at low relative humidity (RH) via chemisorption, resulting in energetically demanding regeneration processes. Metal-organic frameworks (MOFs) are considered promising candidates due to their high uptake capacities and relatively low enthalpies of adsorption.[4] However, the long-term stability of MOFs remains a challenge, with many materials susceptible to degradation under prolonged exposure to moisture, raising concerns about material longevity, metal leaching, and potential health risks.[5]

Porous organic polymers offer a versatile alternative, with broadly tuneable chemistries, high surface areas, and long-term stability, while avoiding the use of scarce or toxic metals. Covalent organic frameworks (COFs), a class of reticular materials, currently make up the majority of organic AWH sorbents.[6,7]

Hypercrosslinked polymers (HCPs), a family of amorphous porous organic polymers, have emerged as promising adsorbents for AWH, offering a scalable and cost-effective alternative to other frameworks. HCPs form densely crosslinked, micro-/mesoporous networks through

View Article Online
DOI: 10.1039/D5NR04338G

Friedel-Crafts chemistry, including self-condensation reactions and the 'knitting' of aromatic compounds using external crosslinkers.[8,9] In 2023, we reported the first HCP for AWH, SHCP-10, a highly sulfonated network capable of adsorbing significant amounts of water even at low relative humidity (0.22 $g \cdot g^{-1}$ at 30% RH) and achieving a total water uptake capacity of 0.81 $g \cdot g^{-1}$ at 25 °C.[10] Sulfonation enhanced water uptake and shifted adsorption onsets to low RH, a strategy that was also effective in imine-linked COFs, underlining the potential of sulfonic acid functionalised networks for AWH.[11,12,13]

Heteroatom incorporation is a widely used strategy to enhance the water uptake performance of adsorbents for AWH. By introducing more electronegative atoms such as oxygen, nitrogen, or sulfur into the polymer backbone, the hydrophilicity of these materials can be significantly improved. For example, Byun et al. synthesised an epoxy-functionalised network via a Diels–Alder reaction, producing an oxygen-rich material with a total uptake capacity of 0.41 $g \cdot g^{-1}$.[14] Similarly, thermal oxidation of HCPs led to the incorporation of various oxygen moieties, resulting in improvements of up to 400% in the networks' total water uptake abilities.[15] Nitrogen incorporation has been particularly effective in enhancing water sorption performance, with many COFs leveraging N-rich backbones to improve water uptake.[16,17] Covalent-triazine frameworks have also demonstrated high water sorption capacities of up to 0.89 $g \cdot g^{-1}$ at 90% RH.[18] Comparably, MOF-303,[19] widely recognised as one of the leading AWH materials, features nitrogen-rich pyrazole units in its backbone, further emphasising the role of heteroatoms in efficient water harvesting materials.

In previous work, we produced a series of HCPs via the crosslinking of fluorene analogues possessing C, N, O, S, or SO_2 in the 9-position with 4,4′-bis(chloromethyl)–1,1′-biphenyl.[20] There, the networks were utilised for the capture of volatile and very volatile organic compounds from complex analyte mixtures. Here, we repurpose these networks for AWH to determine the role of the heteroatoms in water sorption. We subsequently sulfonate the networks to enhance water uptake further and assess how polymer composition impacts post-functionalisation and overall AWH performance. This work aims to illustrate the adaptability of

View Article Online
DOI: 10.1039/D5NR04338G

the networks across distinct application spaces, moving from the capture of pollutants to the generation of clean water from air.

Results and discussion

We synthesised five heteroatom-containing HCPs via the crosslinking of fluorene analogues possessing C, N, O, S, or SO_2 in the 9-position with 4,4′-bis(chloromethyl)–1,1′-biphenyl (Figure 1) following our previous report.[20] The resulting polymers were washed with methanol, dried under vacuum at 80 °C, and obtained in yields of 73-98 % (Table S1). The materials were designated HCP-X, where X denotes the network functionality. Further experimental and synthetic details are provided in Section 1 and 2 of the supporting information (ESI).

The chemical and physical properties of HCP-X were characterised extensively and agree well with our previous work (see Figure 2 and Section 2 of the ESI).[20]

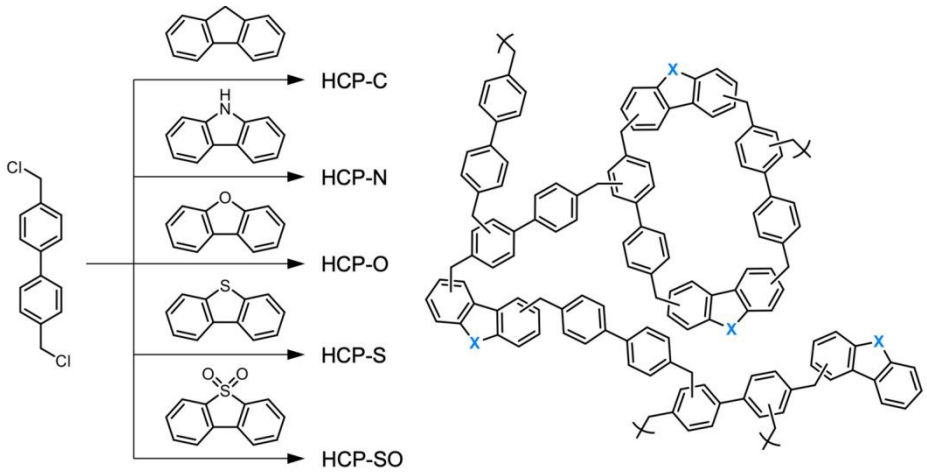

Figure 1. Reaction scheme for the synthesis of hypercrosslinked polymers containing various heteroatoms in their backbones.

We measured N_2 sorption isotherms of all HCPs to probe their textural properties (Figure 2a). All networks exhibited a combination of type I and type IVa isotherms, signifying the presence of micro- and mesopores, respectively.[21] With the exception of HCP-SO, all HCPs showed type H4 hysteresis, indicative of narrow slit-like mesopores. HCP-SO exhibited H2 hysteresis, suggesting the pore structure comprises restricted pore necks, which was attributed to the

View Article Online
DOI: 10.1039/D5NR04338G

incorporation of bulky -SO_2 groups. We confirmed the heterogeneity of the pore structures using QSDFT analysis (Figure 2b), which revealed significant micropore volume and contributions from mesopores of up to 10 nm in diameter.

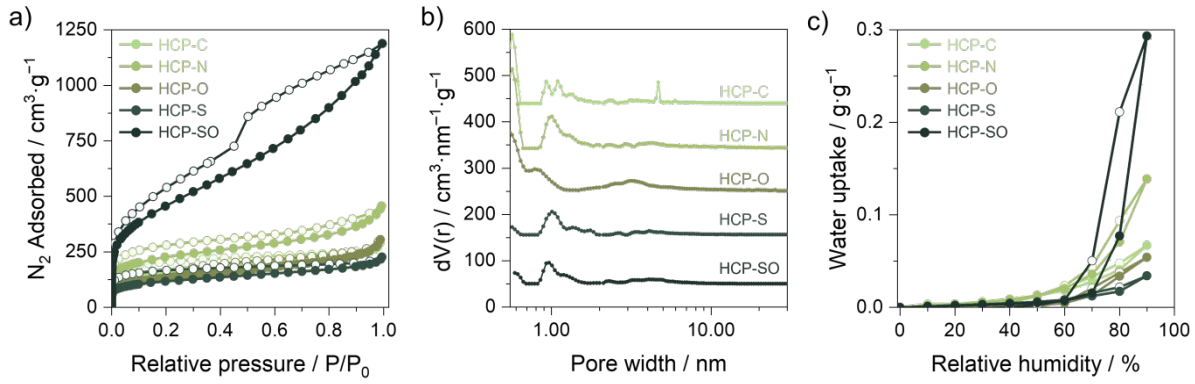

Figure 2. a) N_2 isotherms measured at −196 °C, b) QSDFT pore size distributions, and c) water sorption isotherms (25 °C) of all HCPs. Closed spheres represent uptake and open spheres represent desorption in both nitrogen and water isotherms.

All networks exhibited BET specific surface areas (SSA_{BET}) exceeding 450 $m^2 \cdot g^{-1}$ (Table 1). Network HCP-SO displayed the highest SSA_{BET} of 1590 ± 80 $m^2 \cdot g^{-1}$, potentially due to a reduced incorporation of the fluorene analogue as evidenced by significantly lower yields compared to the other polymers (Table S1).

Table 1. Summary of the porous properties and water sorption of all HCPs, including BET specific surface area, SSA_{BET}, micropore volume, V_{MICRO}, total pore volume, V_{TOT}, and water uptake at 10, 30, and 90% RH at 25 °C. Data was averaged from a sample number, n, of 3 (n = 3).

Sample	SSA_{BET}	V_{MICRO}	V_{TOT}	Water uptake ($g \cdot g^{-1}$)		
	($m^2 \cdot g^{-1}$)	($cm^3 \cdot g^{-1}$)	($cm^3 \cdot g^{-1}$)	10% RH	30% RH	90% RH
HCP-C	550 ± 30	0.12 ± 0.02	0.38 ± 0.01	0.00	0.00	0.07
HCP-N	790 ± 80	0.17 ± 0.01	0.57 ± 0.06	0.00	0.01	0.14
HCP-O	620 ± 10	0.11 ± 0.01	0.45 ± 0.02	0.00	0.00	0.05
HCP-S	450 ± 20	0.09 ± 0.01	0.29 ± 0.01	0.00	0.00	0.03
HCP-SO	1590 ± 80	0.20 ± 0.03	1.62 ± 0.07	0.00	0.00	0.29

We used thermogravimetric analysis (TGA) in air to confirm that all HCPs were stable up to 300 °C (Figure S8). Beyond this temperature, an initial weight increase was observed due to

View Article Online
DOI: 10.1039/D5NR04338G

oxidation, followed by complete degradation at higher temperatures. In a previous study, we demonstrated that thermal oxidation enhanced network hydrophilicity in HCPs, improving their AWH ability.[15]

Dynamic vapour sorption (DVS) analysis was conducted to evaluate the impact of heteroatom moieties on water sorption performance (Figure 2c). Network HCP-C exhibited a total water uptake capacity of just 0.07 $g \cdot g^{-1}$ at 90% RH and 25 °C with an uptake onset at 60% RH. Surprisingly, the introduction of oxygen and sulfur did not enhance hydrophilicity but instead reduced water uptake, with HCP-O and HCP-S achieving 0.05 $g \cdot g^{-1}$ and 0.03 $g \cdot g^{-1}$, respectively. In contrast, the incorporation of amine and sulfone moieties improved water uptake, with HCP-SO displaying the highest total capacity of 0.29 $g \cdot g^{-1}$ at 90% RH and 25 °C.

To rationalise the water sorption behaviour of the HCPs, the underlying adsorption mechanism was examined. Water adsorption generally proceeds via three stages: initial binding of water molecules at hydrophilic sites, water cluster formation and growth, and capillary condensation. The type V water sorption isotherms of heteroatom-containing HCPs indicate the absence of sufficient hydrophilic sites, leading to adsorption dominated by van der Waals interactions.[22,23] Despite adsorption being dominated by weak dispersive interactions, the potential influence of surface chemistry was assessed using logP values and Hansen solubility parameters of the monomers (Table S4). Dibenzothiophene sulfone and carbazole exhibit the highest polarity and hydrogen-bonding parameters, consistent with the water uptake behaviour. In contrast, the trend observed for HCP-C, HCP-O, and HCP-S could not be explained by Hansen solubility and logP alone, as the corresponding monomers show similar values. Differences in their water uptake are instead attributed to variations in the proportion of small-radius micropores (Table 1, Figure 2b). Despite improvements in total water uptake, none of the networks demonstrated significant uptake <30% RH, a key requirement for AWH in arid regions.

Building on the increased water uptake of the heteroatom-containing HCPs and aiming to shift the sorption onset to lower RH, we synthesised sulfonated variants of each network. Our previous work has shown that incorporating sulfonic acid moieties significantly enhances the

View Article Online
DOI: 10.1039/D5NR04338G

water sorption performance of porous organic materials.[10,11] In brief, sulfonated HCPs were produced through a modified literature procedure, replacing $FeCl_3$ with chlorosulfonic acid, which acted as a dual polymerisation catalyst and sulfonation agent.[24] The resulting sulfonated networks (Figure 3a) are named SHCP-X, in accordance with the nomenclature above, where X denotes network functionality. A detailed synthesis description, as well as the corresponding yields (Table S5), is provided in Section 3 of the ESI.

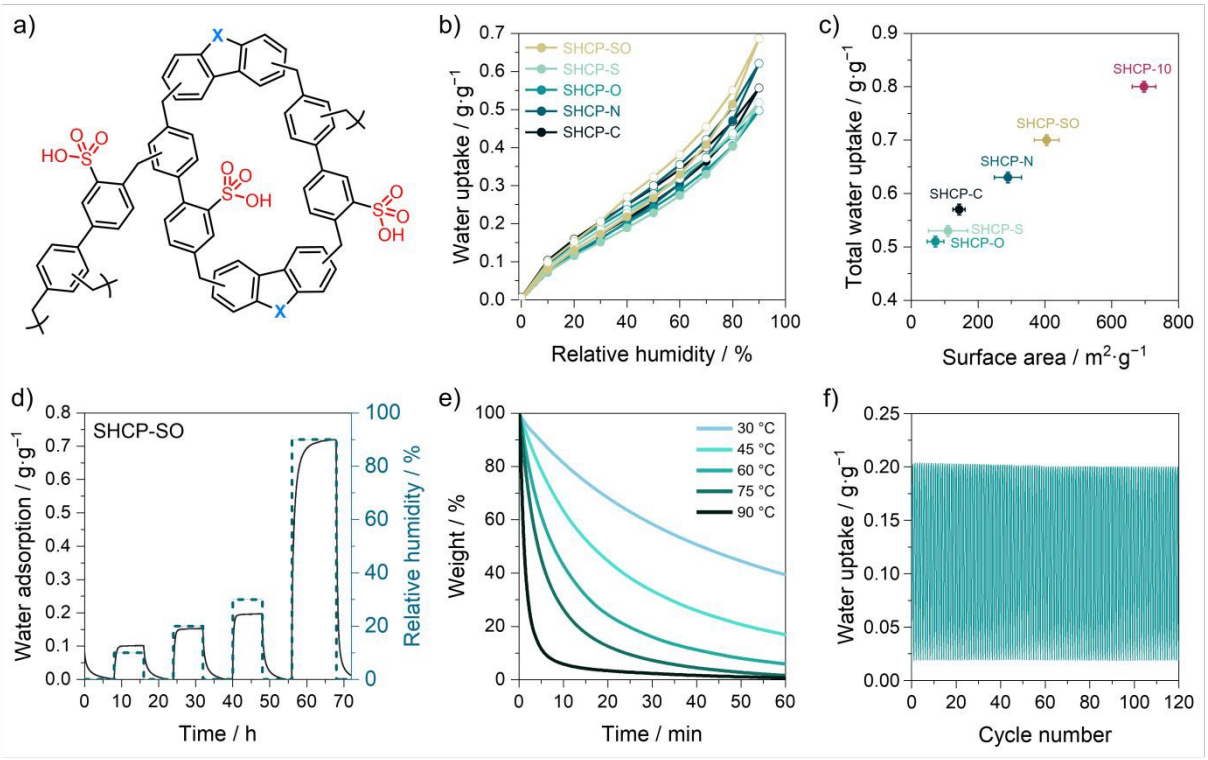

Figure 3. a) Representative structure for SHCP-X. b) Water isotherms at 25 °C. Closed spheres represent uptake and open spheres represent desorption, and c) water uptake plotted against surface area for SHCP-Xs and SHCP-10 from reference 10. d) Water sorption–desorption of SHCP-SO at 10%, 20%, 30%, and 90% RH. e) Desorption of water from SHCP-SO over time at various temperatures, measured using TGA. f) Long-term stability of SHCP-SO over 120 adsorption-desorption cycles consisting of a humidity swing between 0% and 40% RH.

Spectroscopic and physical characterisation confirmed the successful incorporation of sulfonate moieties (Figures S10-S16). In FTIR spectra, new signals at 1345 and 1140 cm^{-1} were assigned to asymmetric and symmetric S=O stretching of sulfonic acid groups, while a C–S stretching peak at 598 cm^{-1} further verified sulfonation. A distinct C–S signal at ~121 ppm was observed in all ssNMR spectra, while high-resolution XPS S 2p spectra displayed a characteristic sulfonic acid peak, with S concentrations reaching up to 5.1 ± 0.1 $mmol \cdot g^{-1}$ in SHCP-SO (Table S6).

View Article Online
DOI: 10.1039/D5NR04338G

Nitrogen sorption isotherms of all SHCPs (Figure S17a) showed reduced uptake and hence lower surface areas compared with their non-sulfonated counterparts due to the introduction of bulky SO_3H groups. All networks exhibited SSA_{BET} >70 $m^2 \cdot g^{-1}$, with SHCP-SO reaching 410 ± 40 $m^2 \cdot g^{-1}$ (Table 2). TGA revealed increased water retention upon sulfonation but a decrease in thermal stability, with degradation onset reduced to ~200 °C (Figure S18).

Table 2. Porous properties and water sorption of SHCP-Xs, including BET specific surface area, SSA_{BET}, micropore volume, V_{MICRO}, total pore volume, V_{TOT}, and water uptake at 10, 30, and 90% RH at 25 °C. (n = 3).

Sample	SSA_{BET} ($m^2 \cdot g^{-1}$)	V_{MICRO} ($cm^3 \cdot g^{-1}$)	V_{TOT} ($cm^3 \cdot g^{-1}$)	Water uptake ($g \cdot g^{-1}$)		
				10% RH	30% RH	90% RH
SHCP-C	140 ± 20	0.04 ± 0.01	0.14 ± 0.02	0.08	0.18	0.57
SHCP-N	290 ± 40	0.06 ± 0.02	0.26 ± 0.04	0.07	0.16	0.63
SHCP-O	70 ± 30	0.02 ± 0.01	0.06 ± 0.01	0.08	0.17	0.51
SHCP-S	110 ± 60	0.02 ± 0.02	0.10 ± 0.04	0.08	0.16	0.53
SHCP-SO	410 ± 40	0.09 ± 0.01	0.23 ± 0.04	0.09	0.18	0.71

Sulfonation significantly enhanced the water sorption behaviour of the heteroatom-containing SHCPs, shifting the uptake onset to lower RH (Figure 3b). At 30% RH, no significant difference was observed between the SHCPs, with uptake ranging from 0.16 to 0.18 $g \cdot g^{-1}$, likely dominated by the hydrophilic sulfonate moieties. Total water uptake also increased across all sulfonated samples, with SHCP-SO achieving the highest total capacity (0.69 $g \cdot g^{-1}$ at 90% RH and 25 °C), and SHCP-O displaying the lowest (0.50 $g \cdot g^{-1}$).

The improved uptake in SHCPs can be rationalised by our proposed water adsorption mechanism in sulfonated porous networks,[25] which is based on work by Shih et al.[26] Initially, single water molecules are adsorbed at sulfonate sites at low RH. Assuming each sulfonic acid group binds one water molecule, the calculated water uptake closely matched the experimental value at 10% RH (Table S7) and highlights the key role of sulfonate groups in low RH water sorption. Further increasing RH leads to cluster growth facilitated by the hydrophilic surface of the sulfonated networks. At >70% RH, these clusters coalesce, leading to capillary condensation within the pores. We analysed correlations between the textural properties and

View Article Online
DOI: 10.1039/D5NR04338G

water sorption behaviour of the SHCP-Xs and SHCP-10[10] to better understand the role of network porosity (Figure 3c, Figure S19). A linear relationship was observed between total water uptake and specific surface area, consistent with our perspective on porous organic polymers for AWH, where a similar trend was identified for COFs.[3] Further correlations of water uptake with micropore volume, total pore volume and sulfonation density (Table S7, Figure S20-21) reveal that water uptake at low RH is governed by the density of highly hydrophilic adsorption sites, whereas at increased RH, the available surface area and pore volume become the dominant factors for uptake, provided a certain threshold hydrophilicity is achieved. .

The water sorption and porous properties of all networks are summarised in Table 2 and compared with examples from the literature in Table S8. SHCP-Xs rank among the top-performing materials for AWH, surpassing several prominent porous adsorbents, including MOFs and COFs. We note that for real-world application, additional tests including the adsorption of contaminants and the assessment of the quality of harvested water are required but are beyond the scope of this study.

Network SHCP-SO was selected as a representative material for a detailed AWH evaluation due to its excellent total water uptake and performance at low RH. The determination of water sorption/desorption kinetics is essential, as rapid cycling increases water yields within a given timeframe. We subjected SHCP-SO to 10%, 20%, 30%, and 90% RH at 25 °C, and monitored water uptake gravimetrically over time (Figure 3d, all SHCP-Xs are provided in Figure S22). SHCP-SO adsorbed 0.72 $g \cdot g^{-1}$ of water following exposure to 90% RH for 8 h. Remarkably, at ≤30% RH, almost complete uptake (0.20 $g \cdot g^{-1}$) occurred within 1 h. Fitting the uptake data at 30% RH and 25 °C to Fick's laws of diffusion, the water diffusivity of SHCP-SO was estimated to be 2.12 x 10^{-9} $m^2 \cdot s^{-1}$. This value is comparable to that reported for SHCP-10 (2.31 x 10^{-9} $m^2 \cdot s^{-1}$),[10] and consistent with the adsorption dynamics expected for polymeric adsorbents, which take up water vapour more rapidly than inorganic adsorbents such as zeolites and MOFs.[27]

View Article Online
DOI: 10.1039/D5NR04338G

To demonstrate the reversibility of water sorption, SHCP-SO was conditioned at ~45% RH and 20 °C for 24 h to allow water adsorption. Subsequently, the water-loaded SHCP-SO was subjected to 30, 45, 60, 75, and 90 °C under dry airflow in the TGA, where desorption was monitored gravimetrically (Figure 3e, all SHCP-Xs are provided in Figure S23). Water desorption commenced at 45 °C, due to the flow of dry air over the sample. Water removal of >80% was achieved for all samples within 10 min at 75 °C, while at 90 °C, almost complete desorption occurred within the same timeframe.

We measured additional water sorption isotherms at 15, 35 and 45 °C to monitor performance over a wide range of temperatures and to calculate the heat of water adsorption (Figure S24). SHCP-SO retained its water uptake at varying temperatures under static conditions, confirming robust adsorption, and the heat of adsorption was estimated to be 45 kJ·mol^{-1}.

Lastly, we performed a long-term performance evaluation of SHCP-SO through repeated adsorption-desorption cycles using either heat or a reduced RH as a desorption trigger. After 120 humidity-swing cycles between 0 and 40% RH (Figure 3f), SHCP-SO exhibited a minimal reduction in working capacity, underscoring its potential for repeated AWH.

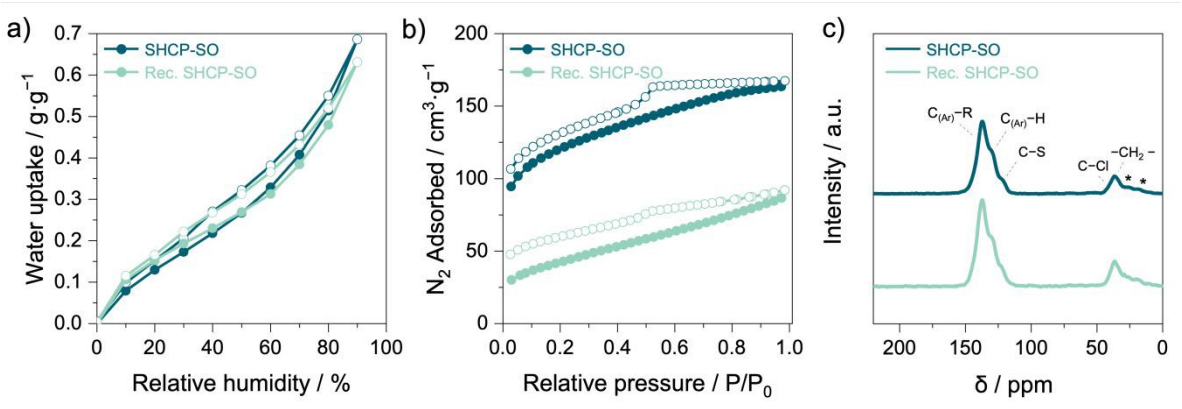

Figure 42. Comparison of SHCP-SO (dark blue) and recovered SHCP-SO after 20 sorption–desorption cycles (cyan, Rec. SHCP-SO), in which desorption was driven by heating at 90 °C for 1 h per cycle. a) Water isotherms measured at 25 °C, b) N_2 isotherms measured at −196 °C. Filled and empty circles represent adsorption and desorption, respectively. c) ^{13}C CP/MAS ssNMR spectra.

View Article Online
DOI: 10.1039/D5NR04338G

To further assess durability under harsher conditions, we subjected all SHCP-X networks to 20 thermal desorption cycles at 90 °C for 1 h per cycle. Post-cycling, SHCP-SO retained its water uptake performance up to 70% RH (Figure 4a) but showed a slight decrease in total uptake capacity at 90% RH to 0.63 $g \cdot g^{-1}$ from 0.69 $g \cdot g^{-1}$. Nitrogen sorption analysis revealed a reduction in the porous properties of SHCP-SO (Figure 4b, Table S9), including a decrease in SSA_{BET} from 405 to 175 $m^2 \cdot g^{-1}$, consistent with the reduction in total water uptake capacity. The textural properties of the other SHCP-X networks did not decrease as significantly (Figure S25). The increased instability in SHCP-SO is consistent with our previous study which reported a reduced thermal stability of HCP-SO.[20] Chemical integrity was maintained across all SHCP-Xs, as confirmed by FTIR, TGA, ssNMR, and XPS (Figure 4c, Figure S26-S28, and Table S10), with no significant changes observed compared to the pristine samples. The absence of a detectable change in SHCP-SO is likely due to the high degree of sulfonation, which masks the spectral regions associated with the sulfone groups.

Conclusion

In this study, we demonstrated the enhancement of hypercrosslinked polymer hydrophilicity via the inclusion of various heteroatoms, improving their atmospheric water harvesting ability. The introduction of nitrogen and sulfone moieties led to an improved total uptake capacity with HCP-SO reaching 0.29 $g \cdot g^{-1}$, while ether and thioether groups did not yield any improvement compared to a non-functionalised HCP (HCP-C). Heteroatom inclusion in the network backbone at the achieved concentration was insufficient in shifting the water uptake onset to ≤30% RH, a critical threshold for adsorption-based atmospheric water harvesting. The additional inclusion of sulfonate groups successfully addressed this limitation, lowering the water uptake onset to <10 % RH and improving the total water uptake capacity. The highest-performing network, SHCP-SO, achieved an impressive total water uptake of 0.69 $g \cdot g^{-1}$ and good performance in drier conditions (0.18 $g \cdot g^{-1}$ at 30% RH and 25 °C). Long-term performance evaluations confirmed the retention of water sorption performance in SHCP-SO,

View Article Online
DOI: 10.1039/D5NR04338G

with no significant changes in chemical composition but some decrease in porosity upon heat cycling. Comparative analysis revealed that the total water uptake capacity of sulfonated HCPs correlated linearly with specific surface area, while performance in drier conditions (30% RH) was solely dependent on the presence and concentration of highly hydrophilic sulfonate groups.

Acknowledgement

The authors acknowledge the funding support of the University of Vienna (Austria). The authors thank Mag. Johannes Theiner and the Microanalytical Laboratory (University of Vienna) for their assistance with elemental analysis and the NMR Centre (University of Vienna) for assistance with ssNMR.

Author contributions

P.S synthesised and characterised HCPs. P.S. and L.P. synthesised and characterised SHCP-Xs, performed water sorption/desorption tests and recycling experiments. P.S and R.T.W. designed experiments. R.T.W. supervised this work. P.S wrote the initial draft of the manuscript. All authors discussed results and edited the manuscript.

Competing Interests

There are no conflicts of interest to declare.

Author Information

Paul Schweng - Institute of Materials Chemistry and Research, Faculty of Chemistry, University of Vienna, 1090, Vienna, Austria; ORCID: 0009-0008-4218-377X. E-mail: paul.schweng@univie.ac.at

Lisa Pammer - Institute of Materials Chemistry and Research, Faculty of Chemistry, University of Vienna, 1090, Vienna, Austria. E-mail: lisa.pammer@univie.ac.at

Assoc.-Prof. Dr. Robert T. Woodward - Institute of Materials Chemistry and Research, Faculty of Chemistry, University of Vienna, 1090, Vienna, Austria; ORCID: 0000-0003-0834-5137. E-mail: robert.woodward@univie.ac.at.

View Article Online
DOI: 10.1039/D5NR04338G

References

[1] United Nations. Sustainable Development Goals Report, 2022, https://unstats.un.org/sdgs/report/2022/ (accessed February 26, 2025).
[2] Gleick, P. Water in Crisis: A Guide to the World's Fresh Water Resources, Oxford University Press, Oxford **1993**, pp. 13–24.
[3] Schweng, P.; Woodward, R. T. Challenging POPular Opinion: Porous Organic Polymers for Atmospheric Water Harvesting. *React. Funct. Polym.* **2024**, *203*, 106014. https://doi.org/10.1016/j.reactfunctpolym.2024.106014.
[4] Kalmutzki, M. J.; Diercks, C. S.; Yaghi, O. M. Metal–Organic Frameworks for Water Harvesting from Air. *Adv. Mater* **2018**, *30* (37), 1704304. https://doi.org/10.1002/adma.201704304.
[5] Burtch, N. C.; Jasuja, H.; Walton, K. S. Water Stability and Adsorption in Metal–Organic Frameworks. *Chem. Rev.* **2014**, *114* (20), 10575–10612. https://doi.org/10.1021/cr5002589.
[6] Grunenberg, L.; Savasci, G.; Emmerling, S. T.; Heck, F.; Bette, S.; Cima Bergesch, A.; Ochsenfeld, C.; Lotsch, B. V. Postsynthetic Transformation of Imine- into Nitrone-Linked Covalent Organic Frameworks for Atmospheric Water Harvesting at Decreased Humidity. *J. Am. Chem. Soc.* **2023**, *145* (24), 13241–13248. https://doi.org/10.1021/jacs.3c02572.
[7] Mou, K.; Meng, F.; Zhang, Z.; Li, X.; Li, M.; Jiao, Y.; Wang, Z.; Bai, X.; Zhang, F. Pyridazine-Promoted Construction of Vinylene-Linked Covalent Organic Frameworks with Exceptional Capability of Stepwise Water Harvesting. *Angew. Chem. Int. Ed.* **2024**, *63* (34), e202402446. https://doi.org/10.1002/anie.202402446.
[8] Wood, C. D.; Tan, B.; Trewin, A.; Niu, H.; Bradshaw, D.; Rosseinsky, M. J.; Khimyak, Y. Z.; Campbell, N. L.; Kirk, R.; Stöckel, E.; Cooper, A. I. Hydrogen Storage in Microporous Hypercrosslinked Organic Polymer Networks. *Chem. Mater.* **2007**, *19* (8), 2034–2048. https://doi.org/10.1021/cm070356a.
[9] Li, B.; Gong, R.; Wang, W.; Huang, X.; Zhang, W.; Li, H.; Hu, C.; Tan, B. A New Strategy to Microporous Polymers: Knitting Rigid Aromatic Building Blocks by External Cross-Linker. *Macromolecules* **2011**, *44* (8), 2410–2414. https://doi.org/10.1021/ma200630s.
[10] Schweng, P.; Mayer, F.; Galehdari, D.; Weiland, K.; Woodward, R. T. A Robust and Low-Cost Sulfonated Hypercrosslinked Polymer for Atmospheric Water Harvesting. *Small* **2023**, *19* (50), 2304562. https://doi.org/10.1002/smll.202304562.
[11] Schweng, P.; Li, C.; Guggenberger, P.; Kleitz, F.; Woodward, R. T. A Sulfonated Covalent Organic Framework for Atmospheric Water Harvesting. *ChemSusChem* **2024**, *17* (20), e202301906. https://doi.org/10.1002/cssc.202301906.
[12] Liu, Y.; Zhu, Y.; Mao, Q.; Chen, W. Enhanced Hydrophilicity of DAAQ-TFP COFs via Sulfonate Modification for Air Water Harvesting in Arid Environment. *Small* **2024**, *20* (51), 2406803. https://doi.org/10.1002/smll.202406803.
[13] Shi, Z.; Guo, Y.; Zou, X.; Zhang, J.; Chen, Z.; Shan, M.; Zhang, Z.; Guo, S.; Yan, F. Low Evaporation Enthalpy Ionic Covalent Organic Frameworks for Efficient Atmospheric Water Harvesting at Low Humidity. Angew. Chem. Int. Ed. Accepted article, e202420619. https://doi.org/10.1002/anie.202420619.
[14] Byun, Y.; Coskun, A. Epoxy-Functionalized Porous Organic Polymers via the Diels–Alder Cycloaddition Reaction for Atmospheric Water Capture. *Angew. Chem. Int. Ed*. **2018**, *57* (12), 3173–3177. https://doi.org/10.1002/anie.201800380.

View Article Online
DOI: 10.1039/D5NR04338G

[15] Schweng, P.; Präg, L.; Woodward, R. T. Regulating the Hydrophilicity of Hyper-Cross-Linked Polymers via Thermal Oxidation for Atmospheric Water Harvesting. *ACS Appl. Mater. Interfaces* **2024**, *16* (43), 58566–58572. https://doi.org/10.1021/acsami.4c11013.
[16] Stegbauer, L.; Hahn, M. W.; Jentys, A.; Savasci, G.; Ochsenfeld, C.; Lercher, J. A.; Lotsch, B. V. Tunable Water and CO2 Sorption Properties in Isostructural Azine-Based Covalent Organic Frameworks through Polarity Engineering. *Chem. Mater.* **2015**, *27* (23), 7874–7881. https://doi.org/10.1021/acs.chemmater.5b02151.
[17] Nguyen, H. L.; Gropp, C.; Hanikel, N.; Möckel, A.; Lund, A.; Yaghi, O. M. Hydrazine-Hydrazide-Linked Covalent Organic Frameworks for Water Harvesting. *ACS Cent. Sci.* **2022**, *8* (7), 926–932. https://doi.org/10.1021/acscentsci.2c00398.
[18] Huang, J.; Yang, Y.; Chen, L.; Zhang, Z.; Xiang, S. Atmospheric Water Harvesting in Microporous Organic Polymers Constructed from Trazine and Benzimidazole Units. *ZAAC* **2023**, *649* (19), e202300167. https://doi.org/10.1002/zaac.202300167.
[19] Hanikel, N.; Prévot, M. S.; Fathieh, F.; Kapustin, E. A.; Lyu, H.; Wang, H.; Diercks, N. J.; Glover, T. G.; Yaghi, O. M. Rapid Cycling and Exceptional Yield in a Metal-Organic Framework Water Harvester. *ACS Cent. Sci.* **2019**, *5* (10), 1699–1706. https://doi.org/10.1021/acscentsci.9b00745.
[20] Schweng, P.; Rippatha, E.; Schwarzinger, C.; Woodward, R. T. Hypercrosslinked Polymers for Volatile and Very Volatile Organic Compound Capture Beyond Commercial Benchmarks, *Angew. Chem. Int. Ed.* **2025**, Early View, e202513362. https://doi.org/10.1002/anie.202513362
[21] Thommes, M.; Kaneko, K.; Neimark, A. V.; Olivier, J. P.; Rodriguez-Reinoso, F.; Rouquerol J.; Sing, K. S. W. Physisorption of gases, with special reference to the evaluation of surface area and pore size distribution (IUPAC Technical Report), *Pure Appl. Chem.*, **2015**, *87*, 1051–1069. https://doi.org/10.1515/pac-2014-1117.
[22] Yang, Q.; Sun, P. Z.; Fumagalli, L.; Stebunov, Y. V.; Haigh, S. J.; Zhou, Z. W.; Grigorieva, I. V.; Wang, F. C.; Geim, A. K. Capillary Condensation under Atomic-Scale Confinement, *Nature* **2020**, *588* (7837), 250–253. https://doi.org/10.1038/s41586-020-2978-1.
[23] Oppenheim, J. J.; Dincă, M. Isoreticular Curves: A Theory of Capillary Condensation To Model Water Sorption within Microporous Sorbents. *J. Am. Chem. Soc*. **2024**, *146* (30), 20615–20626. https://doi.org/10.1021/jacs.4c02743.
[24] Blocher, A.; Mayer, F.; Schweng, P.; Tikovits, T. M.; Yousefi, N.; Woodward, R. T. One-Pot Route to Fine-Tuned Hypercrosslinked Polymer Solid Acid Catalysts. *Mater. Adv.* **2022**, *3* (15), 6335–6342. https://doi.org/10.1039/D2MA00379A.
[25] Schweng, P.; Naryshkina, A.; Glabonjat, R. A.; Woodward, R. T. Scalable Sulfonated Activated Carbons as High-Capacity Sorbents for Atmospheric Water Harvesting. *Carbon* **2026**, *247*, 120964. https://doi.org/10.1016/j.carbon.2025.120964.
[26] Shih, S.-M.; Lin, L.-C. Water Adsorption in Metal–Organic Frameworks: Characteristics, Mechanisms, and Structure–Property Relationships. *J. Am. Chem. Soc.* **2025**, *147* (38), 34791–34803. https://doi.org/10.1021/jacs.5c10686.
[27] Zhong, Y.; Zhang, L.; Li, X.; El Fil, B.; Díaz-Marín, C. D.; Li, A. C.; Liu, X.; LaPotin, A.; Wang, E. N. Bridging Materials Innovations to Sorption-Based Atmospheric Water Harvesting Devices. *Nat. Rev. Mater.* **2024**, *9* (10), 681–698. https://doi.org/10.1038/s41578-024-00665-2.

View Article Online
DOI: 10.1039/D5NR04338G

The data supporting this article have been included as part of the Supplementary Information. Supplementary Information: experimental methods, synthesis and characterisation data, tables summarising yields, elemental composition and textural properties, spectroscopic data (FTIR, solid-state NMR, XPS), gas and water sorption measurements, and additional figures supporting the discussion.